encit 2020

ABCM Associação Brasileira de Engenharia e Ciências Mecânicas

18th Brazilian Congress of Thermal Sciences and Engineering
November 16-20, 2020 (Online)

ENC-2020-0634
FORECASTING THE LENGTH OF THE THERMAL DEVELOPING REGION AT THE ENTRANCE OF BIFURCATIONS

Flavio Peres Amado
Universidade Estacio de Sá, Rua Eduardo Luiz Gomes, 134 - Morro do Estado, Niterói - RJ, 24020-340
e-mails: flavioam@petrobras.com.br; fpamado@live.estacio.com.br
Mila Rosendarl Avelino
Universidade do Estado do Rio de Janeiro – UERJ, Cx. Postal 68503, Rio de Janeiro - RJ, 21945-970;
e-mail: mila.avelino@pq.cnpq.br
Jordana Colman
Universidade Federal do Rio de Janeiro – UFRJ, Centro de Tecnologia - Av. Horácio Macedo, 2030, Cidade Universitária, Rio de Janeiro - RJ, 21941-450
e-mail: jordanacolman@yahoo.com.br
Ediomedson Sales de Lucena
Universidade Federal Fluminense, Rua Passo da Pátria, 152 – 470, São Domingos, Niterói - RJ, 24210-240 e-mails: *ediomedson@hotmail.com*

Abstract. *In this work the region of thermal development at the entrance of asymmetric bifurcations is approached. Measurements of the length of this stretch are performed on images generated by numerical simulation, executed with the aid of the finite difference method, as well as a commercial simulator. The objective is to draw equations that can predict the extension as a function of diameter and dimensionless quantities such as Dean and Prandtl numbers. Three equations are proposed that deal with the isolated variation of the flow rate, the angles of the bifurcation, as well as the diameter of the feeder channel. These expressions. are also tested as a wide-aspect equation, that is, a correlation that could predict the extension of the not developed thermal region with the variation of all dimensional and flow characteristics together. The study considers that the proposed equations are valid for symmetric and asymmetric bifurcations. Subsequent work is recommended where the behavior of the thermal development is verified as a function of physical properties like density and viscosity, which make up the Reynolds number*

Keywords: *Thermal development, bifurcations*

1. INTRODUCTION

In the last three years, the authors have developed works that intend to predict the extension of the so-called region of flow development in symmetric and asymmetric bifurcations of microchannels and conventional pipes under laminar flow. Thus, six manuscripts (three full papers and three abstracts) were submitted, approved, presented and published in important national and international conferences, multi-thematic and specific to mechanical sciences (Amado et al, 2017, Amado et al., 2018a Amado et al, 2018b, Amado et al, 2018c, Amado et al, 2018d, and Amado 2018e). In addition, the authors submitted to COBEM 2019 a fourth paper (Amado et al, 2019), which intended to test the same equations for the flow of oils with very low Reynolds number values, involving variations in density and viscosity. The present proposal intends to enlarge the state-of-the-art, investigating now the region of thermal development of laminar flows in bifurcations.

According to Ghobadi and Muzychka, 2016, in an excellent review of correlations describing the pressure drop and heat transfer in laminar flow through curved ducts, up to the publication date of their work, there were very few equations that set out to describe the size of the thermal developing region in toroidal geometries. In this way, it becomes absolutely legitimate and necessary a work of surveying equations for this purpose.

Initially, Janssen and Hoogendoorn, 1978, proposed an expression in the format shown in Eq. (1), which aims to describe the length of that region at the entrance of helical tubes, under boundary conditions that address constant transverse heat flux and constant peripheral temperature at the wall, in stretches of developed flow but still undergoing thermal development.

$$L_{th} = \frac{15.7Pr^{-0.8}}{De} \tag{1}$$

Additionally, for concomitant conditions of flow and thermal development, they established Eq. (2) below.

$$L_{th} = \frac{20Pr^{0.2}}{De} \tag{2}$$

In both equations, *Pr* is the Prandtl number and *De*, the Dean number, classically defined in Eq. (3), where *Re* is the Reynolds number, *R* the radius of curvature of the helicoid and *a*, the inner radius of the tube.

$$De = Re\sqrt{\frac{a}{R}} \tag{3}$$

Since a bifurcation is not exactly a curved geometry, in Amado et al, 2018b, *R* is defined as the radius of the arc containing the feeder channel of the bifurcation and one of the fork outlets, and is determined by Eq. (4).

$$R = \frac{1200.5DRe^{0.66}}{\theta^2} \tag{4}$$

Here, *D* is the diameter or hydraulic diameter of the bifurcation pipe, and θ the half angle of the fork.

Equations (1) and (2) were corroborated by Yao, 1984, and indicate that the length L_{th}, of the thermal developing region is primarily influenced by the secondary flow generated in the curve and somewhat less by thermal diffusivity, which is the main determining factor in straight stretches.

Later, Liu and Masliyah, 1994, under conditions of simultaneity of thermal and flow development, proposed a more complex formulation, evidenced in Eq. (5) below:

$$L_{th} = \frac{0.155+0.0064De^{0.5}Pr^{0.25}}{1+0.0122DePr}Pr \tag{5}$$

According to them, this equation is valid for $0.01<(R/a)<0.15$ and $20<De<5000$.

2. MATERIALS AND METHODS

Considering the above, the primary proposal of the research is the lifting of correlations in the formats shown in Eq. (6) and (7), aiming at the prediction of the length of the not developed thermal region, L_{th}, under conditions of simultaneity of flow and thermal development in bifurcations, with variation of angles, flow rates and diameters of channel, separately.

$$L_{th} = \frac{c1Pr^{c2}}{De^{c3}} \tag{6}$$

$$L_{th} = \frac{c4+c5D^{\ c6}Pr^{c7}}{c8+c9DePr}Pr \tag{7}$$

Where *c1* to *c9* are constants to be raised by measurements in images generated in CFD simulations by finite differences and through a commercial CFD package, which work with finite elements, as well as by mathematical iterations.

Beyond that, it is necessary to observe that equations in the format of Eq. (6) and (7) must be also tested with variation of angles, flow rates and diameters of channel simultaneously, so that a wide-reaching expression, i.e., an expression that translates in itself the variation of all the parameters which influence the phenomenon, be established. If these correlations are not suitable for wide aspect, a new option should be lifted.

It is important to note that, according to Amado et al., 2019, symmetric bifurcations are specific cases of asymmetric bifurcations, and therefore, equations proposed herein, are valid for any angular composition of bifurcations, within the flow rates and diameters in which the simulations were performed. Thus, a standard asymmetrical bifurcation with half angles $\theta_1 = 45º$ and $\theta_2 = 30º$ was employed. The fork was designed as a steel tube with a wall thickness of 1 mm and a conductivity of 80 W/mK. The flow rate was varied according to Tab. 1, the half-angles of the asymmetric bifurcation, as shown in Tab. 2, with the diameter of the bifurcation tube varying as stated by Tab. 3.

As in the methodology developed and applied in Amado et al 2018a, the simulated images from the commercial package served as reference for the simulation in finite differences. It was just for the comparison of the shape.

2.1 Simulation Strategy and Boundary Conditions

The simulation strategy used in the present work is similar to that employed in the previous works by the same authors (Amado et al, 2018a, b, c), however, involving the energy equation, since in those articles, the interest was only the survey

of the velocity fields and here, it extends to the temperature gradients. Thus, simulations were performed in structured programming, considering that the outlets of the bifurcation are separated into two independent stretches and, consequently, a not very robust simulation method is sufficient, given the low complexity of the geometry.

Table 1. Conditions of flow rate in asymmetric bifurcations with the same pair of half-angles and diameter.

Channel	Dimensional data	Flow rate at the feeder channel inlet (m^3/s)
Inlet 1	Half-angles θ_1 and θ_2 as 45º and 30º, for bifurcations with 0.02 m in diameter and 0.9 m of length.	5.56×10^{-11}
Inlet 2		6.95×10^{-11}
Inlet 3		1.11×10^{-10}
Inlet 3'		1.11×10^{-10} ($\theta_1 = 60º$ and $\theta_2 = 45º$)
Inlet 4		1.39×10^{-10}
Inlet 5		1.81×10^{-10}
Inlet 6		2.78×10^{-10}

Table 2. Variation of half-angles in asymmetric bifurcations with constant flow rate and diameter.

Channel	Half-angles (grades)	Flow conditions and dimensions
Left outlet 7	5	1.39×10^{-10} m^3/s of flow rate at the feeder channel inlet, for bifurcations with 0.02 m in diameter and 0.9 m of length.
Right outlet 7	15	
Left outlet 8	15	
Right outlet 8	30	
Left outlet 9	30	
Right outlet 9	45	
Left outlet 10	45	
Right outlet 10	60	
Left outlet 11	60	
Right outlet 11	75	
Left outlet 12	75	
Right outlet 12	90	

Table 3. Values for the case of variation of diameters.

Channel	Diameter (m)	Flow Condition and angles
Left outlet 13	0.010	1.39×10^{-10} m^3/s of flow rate at the feeder channel inlet and half-angles θ1 and θ2 as 45º and 30º
Right outlet 13	0.010	
Left outlet 14	0.015	
Right outlet 14	0.015	
Left outlet 15	0.020	
Right outlet 15	0.020	
Left outlet 16	0.025	
Right outlet 16	0.025	
Left outlet 17	0.030	
Right outlet 17	0.030	
Left outlet 18	0.035	
Right outlet 18	0.035	

Boundary conditions and assumptions were:

- Velocity at the inlet is established by Eq. (8), where Q is the fluid flow rate (water at 80 ºC and under atmospheric pressure), a is the radius of the channel and r is the distance from the central axis to the node to be calculated;
- Velocity equal to zero near the inner wall;
- Constant heat flow through walls;

- Constant peripheral temperature at the wall;
- The air composes the external environment, with a convection coefficient of 1.2 W/m^{2}K;
- The water flowing internally presents a convection coefficient of 2.5 W/m^{2}K.

With this in mind, Navier-Stokes Eq. (9) to (11) and Energy Eq. (12) and (13) were discretized in finite differences and computationally implemented. The convergence criterion was 10^{-8}, compared to the relative error and the simulated time interval was 1 s, with time steps of 10^{-6} s. In mesh terms, the z-direction was established as axial, with a non-uniform structured distribution, with 60 lines in the initial 2% of the conduit and 200 lines in the remaining 98%. The x direction was agreed as transversal, with a uniform structured distribution of 1200 divisions. This structuring allowed to concentrate the mesh at the beginning of the bifurcation and to gain processing time, in such a way that each simulation spent a total of approximately 15 hours. Fig. 1 shows (a) the mesh generated in artisanal programming, which used finite differences, as well as (b) that generated in the commercial package.

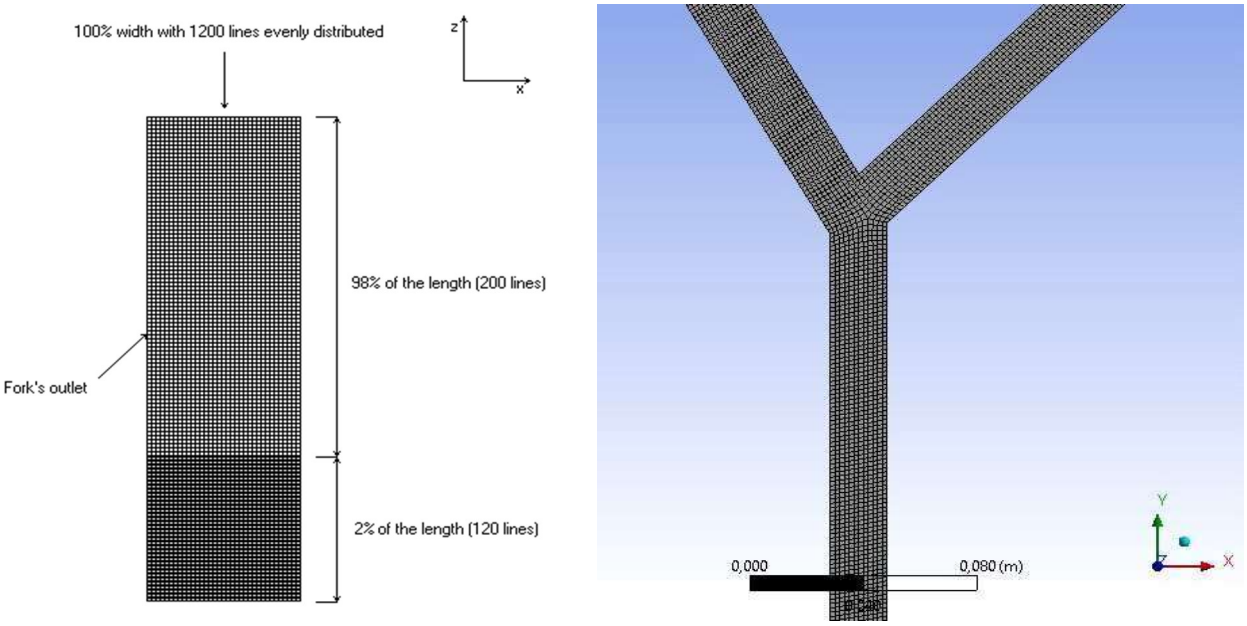

(a) (b)

Figure 1. (a) Sketch of the mesh developed in the handmade model (in house code) and (b) Mesh generated automatically by the commercial package, where 21041 nodes and 19408 elements were developed

$$v_{axial} = \pm \cos\theta_i \frac{2Q}{\pi r^4}(a^2 - r^2) \tag{8}$$

Equation for mass conservation:

$$\frac{\partial v_x}{\partial x} + \frac{\partial v_y}{\partial y} = 0 \tag{9}$$

x Momentum:

$$\rho\left(\frac{\partial v_x}{\partial t} + v_x\frac{\partial v_x}{\partial x} + v_z\frac{\partial v_x}{\partial z}\right) = \rho g_x - \frac{\partial P}{\partial x} + \mu\left(\frac{\partial^2 v_x}{\partial x^2} + \frac{\partial^2 v_x}{\partial z^2}\right) \tag{10}$$

z Momentum:

$$\rho\left(\frac{\partial v_z}{\partial t} + v_x\frac{\partial v_z}{\partial x} + v_z\frac{\partial v_z}{\partial z}\right) = \rho g_z - \frac{\partial P}{\partial z} + \mu\left(\frac{\partial^2 v_z}{\partial x^2} + \frac{\partial^2 v_z}{\partial z^2}\right) \tag{11}$$

Energy Equation:

$$\rho C_p\left(\frac{\partial T}{\partial t} + v_x\frac{\partial T}{\partial x} + v_y\frac{\partial T}{\partial y}\right) = kfluido\left(\frac{\partial^2 T}{\partial x^2} + \frac{\partial^2 T}{\partial y^2}\right) + \mu\phi \tag{12}$$

Where,

$$\phi = 2\left[\left(\frac{\partial v_x}{\partial x}\right)^2 + \left(\frac{\partial v_y}{\partial y}\right)^2\right] + \left(\frac{\partial v_x}{\partial y} + \frac{\partial v_y}{\partial x}\right)^2 \quad (13)$$

3. RESULTS AND DISCUSSION

Measurements of the length L_{th} were made on the images generated in the simulations. As examples, Fig. 2a shows the simulation of the thermal flow through the commercial code, for water at 80 ºC, under atmospheric pressure, in a bifurcation with flow rate of 1.39 x 10^{-10} m^3/s. Fig 2b shows the same phenomenon, but in the image "in close" generated by simulation via finite differences for the half-angle of 30º and how the measurements were performed. Fig. 3a and b show thermal gradient images for the bifurcation 16 (Tab. 3 - feeding channel diameter of 0.025 m), respectively generated by the commercial package and by the finite difference method.

With these measured values, the best approximation obtained for the flow rate variation was that indicated as Eq. (14) and for angular variation was Eq. (15).

$$L_{th} = \frac{3.3x10^{-8} + 6.4x10^{-8} De^{0.5} Pr^{0.25}}{1 + 0.0122 DePr} Pr \quad (14)$$

$$L_{th} = \frac{0.00035 Pr^{0.2}}{De^{-0.04}} \quad (15)$$

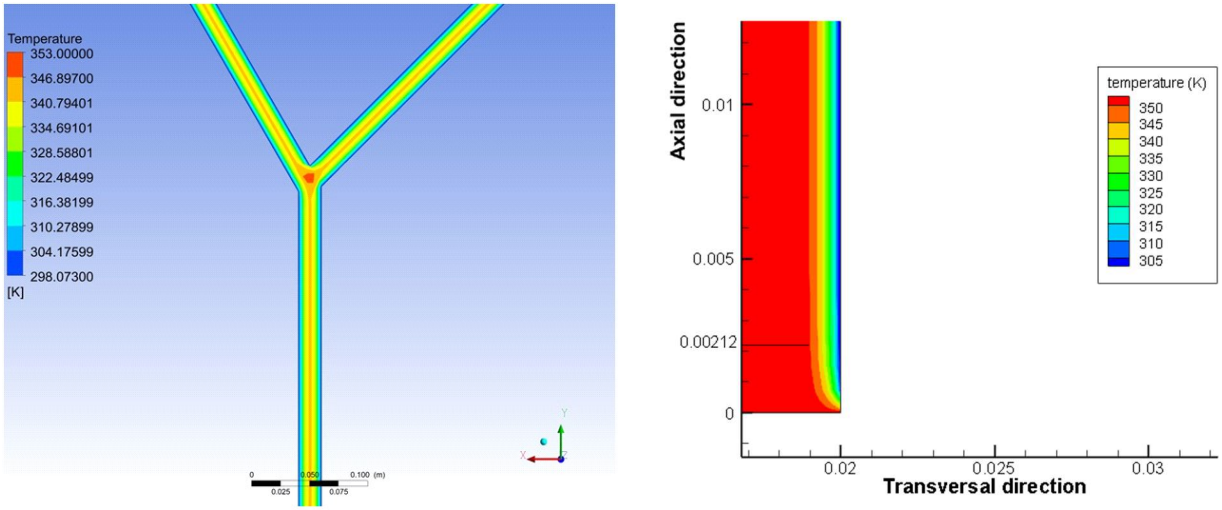

(a) (b)

Figure 2. (a) Temperature gradient for water flowing at 80 ºC and under atmospheric pressure, at the inlet 3, with 0.02 m in diameter, flow rate 1.39 x 10^{-10} m^3/s. Image generated by the commercial code; (b) Temperature gradient for water flowing at 80 ºC and under atmospheric pressure, at the inlet 3, with 0.02 m in diameter, half-angle of 30º, flow rate 1.39 x 10^{-10} m^3/s. Image generated by the finite difference method.

Figures 4 and 5 compose a plot of the values of flow rate variation and variation of half-angles, respectively. Although some scattering occurs, values of L_{th} for flow rate variation, tended to decrease with increasing flow rate, which does not compose intuitive behavior, since flow rate values seem, in a primary analysis, lead to higher L_{th} values. However, Eq. (14) presents Dean Number in the denominator, which shows that the extension of the undeveloped thermal region may decrease with flow rate. This fact gives meaning to the aspect of Fig. 4, which shows decreasing values.

Comparison of values in Fig. 5, show that the larger the bifurcation angle, the higher the thermal developing region. This conclusion is corroborated by Okuyade and Abbey, 2016, studying thermal flows in symmetrical bifurcations with rectangular section. However, results presented herein show a very tenuous variation and very small absolute values, but this behavior is also ratified in the literature, when the flow developing region is reported. Ghobadi and Muzychka, 2016, citing several references, have shown that under conditions of thermally developing and hydrodynamically developed flow, for both experimental data (Cheng and Akiyama, 1970), and numerical studies (Dravid et al, 1971, Tarbell,and Samuels, 1973, Janssen and Hoogendoorn, 1978, Choi et al, 1979, Stewartson et al, 1980, Stewartson et al, 1982, Soh, 1983, So et al, 1991, Ebadian et al, 2000), the length of the thermal development in flows initiated in curves are 20 to 50% smaller than in those initiated in straight stretches. Gongnan et al., 2014 and Amado et al., 2018a, b, c, also found

regions of undeveloped flow quite small for bifurcations at various angles. Considering that the thermal gradient is dependent on the velocity field, it is to be expected that the not thermally developed region be also small.

Equations (14) and (15) were also tested for the diameter variation. Figure 6 shows amounts calculated compared to those measured. This figure presents a poor coincidence of values, mainly because the measurements of L_{th} were quite scattered. In this way, Eq. (16) is proposed only for these cases, whose comparison of values is shown in Fig. 7.

$$L_{th} = \frac{1.8x10^{-8}+6.4x10^{-8}De^{0.5}Pr^{0.25}}{0.25+\ .0488DePr}Pr \tag{16}$$

Results of Eq. (16) present better coincidence for smaller diameters. The fact is that measurements on images taken from computational simulations behave like experimental measurements, in the sense of being subject to scattering. Thus, values read for the largest diameters fled from a pattern of increase of L_{th} obtained with the smallest ones. It is suggested to work on new simulations, with more accurate measurements. In any case, Eq. (16) fits more acceptably to the present results than Eq. (14) and (15).

Taking into account all the results measured and presented herein, Fig. 8 shows the comparison with those calculated by Eq. (14), (15) and (16). The initial part of the graph refers to L_{th} values for flow rate variation, the intermediate part refers to the angular variation and the final part deals with the variation of channel diameter.

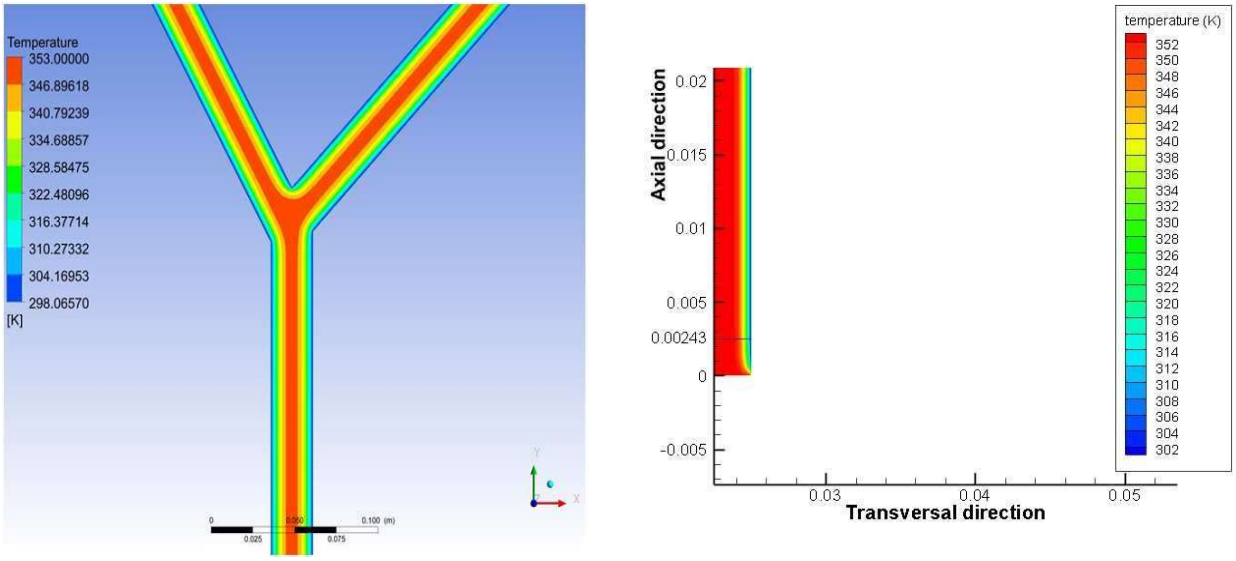

(a) (b)

Figure 3. (a) Bifurcation 4, feeder channel diameter of 0.025 m, water flowing at 80 ºC and atmospheric pressure. Simulation through the commercial code; (b) Outlet of the bifurcation 4 "in close", half-angle of 45 °, feeder channel diameter of 0.025 m, with water flowing at 80 ° C and atmospheric pressure. Simulation through finite differences.

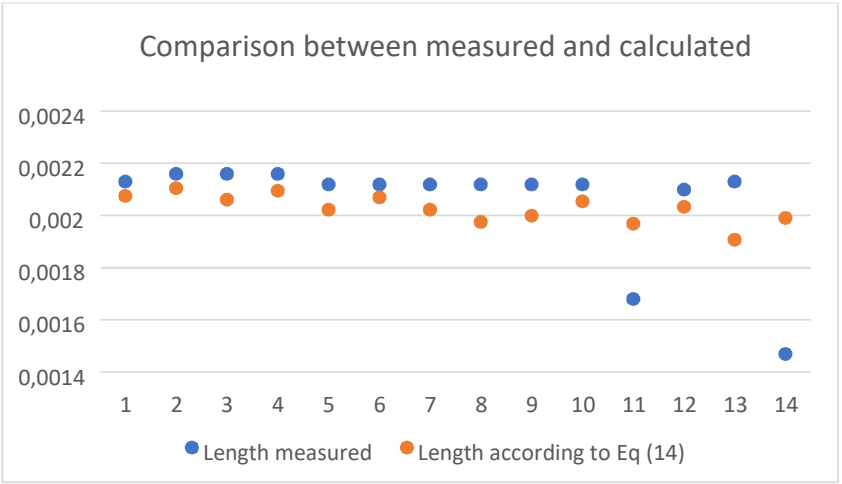

Figure 4. L_{th} values measured in images that simulate flow rate variation versus values calculated by Eq. (14)

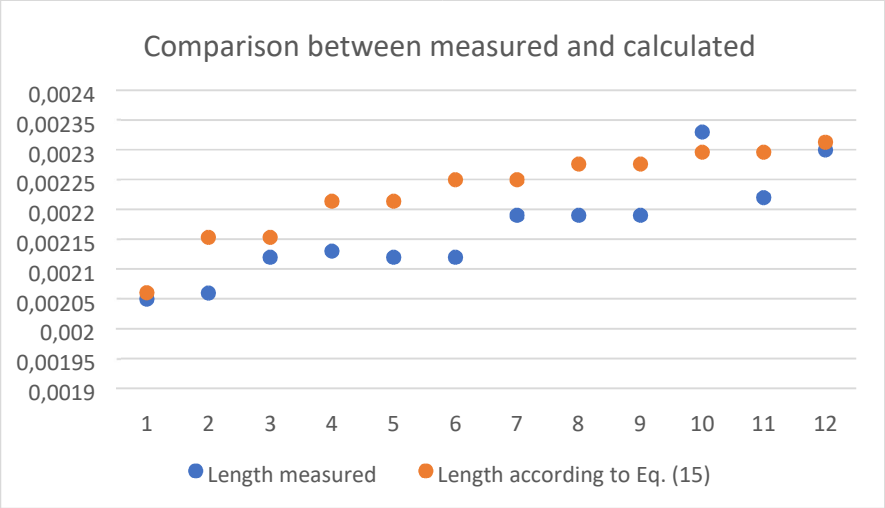

Figure 5. L_{th} values measured in images that simulate angular variation versus values calculated by Eq. (15)

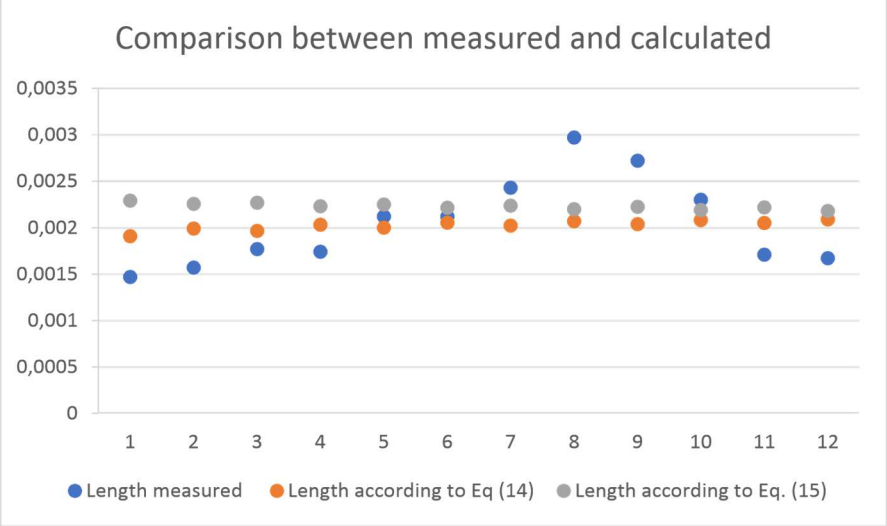

Figure 6. Comparison of measured results and values calculated by Eq. (14) and (15), under conditions of prediction of L_{th} as a function of channel diameter.

By and large, the tendency is to increase the length of the thermal developing region with the general increase of the tested variables. Notwithstanding, the scattering of measured values was not negligible. Eq. (15) fits these values better than Eq. (16), but is not as coincident. In this way, Eq. (14) is presented as the most adequate for a broad-looking expression, reasonably well covering the variation of all parameters considered in this work, within the tested range, i.e., 5.56×10^{-11} m/s $< Q < 2.78 \times 10^{-10}$ m/s, $5^o < (\theta 1$ and $\theta 2) < 90^o$ and 0.01m $< D <$ 0.035m.

As extra observation and just for the sake of didactics, it is important to highlight that the shape of the Eq. (15) is exactly that presented by Janssen and Hoogendoorn, 1978. However, a format similar to that employed by Springer et al., 2009, which is the same one used in previous works by the present authors, would be more appropriate. In this case, Eq. (15) will be rewritten according to Eq. (17).

$$L_{th} = 0.00035 Pr^{0.2} De^{0.04} \tag{17}$$

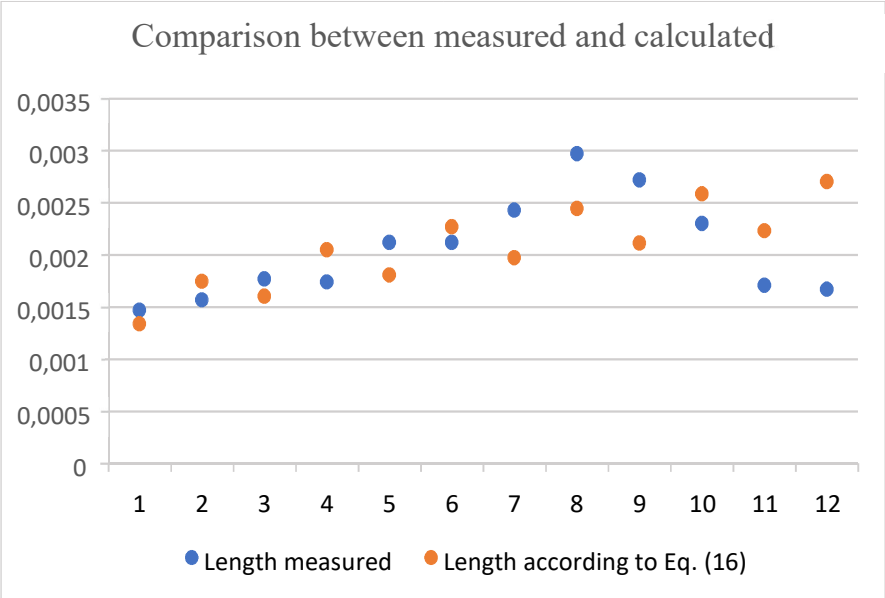

Figure 7. Comparison of L_{th} values measured and calculated by Eq. (16), for variation of feeder channel diameter.

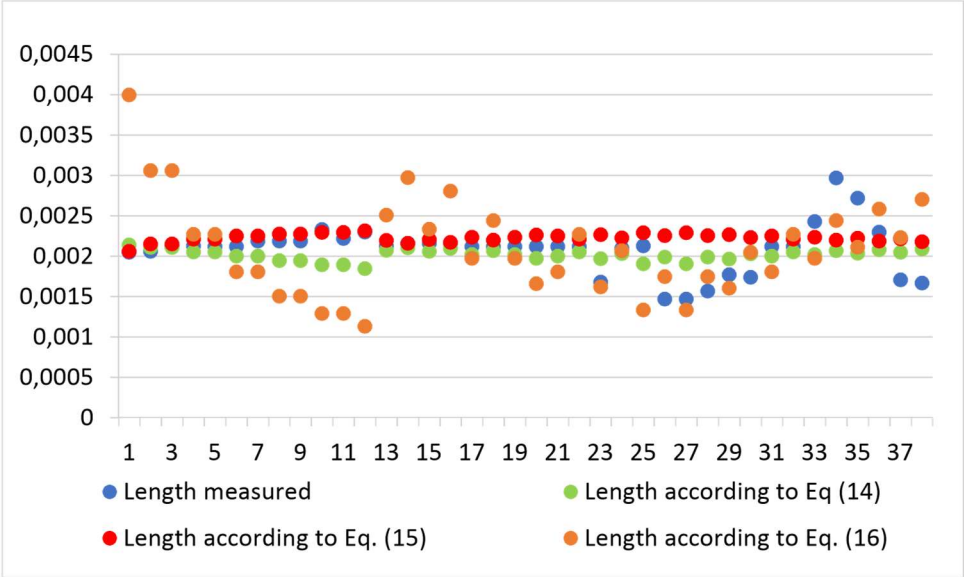

Figure 8. Comparison between measured and calculated values for L_{th} in bifurcations with variation of flow rate, haf-angle and diameter, according to Eq. (14), (15) and (16).

Finally, it is important to evince that the present study further recommend a subsequent work of testing the behavior of thermal developing region in bifurcations as a function of the variation of physical properties that make up the Reynolds number, in the same way as previously elaborated in Amado et al, 2019, for the undeveloped flow region.

4. CONCLUSIONS

The thermal developing region at the entrance of asymmetric bifurcations was verified in an approach similar to that used by the authors regarding the region of flow development. Equations in formats proposed in the literature were raised through the reading in images generated via finite differences. So far, it has been possible to verify results from measurements in tests simulating the flow rate variation in the feeder channel of the bifurcation, as well as the angle and diameter variations.

At this point, it is possible to state that the expression in the form $L_{th} = \frac{3.3x10^{-8}+6.4x10^{-8}De^{0.5}Pr^{0.25}}{1+0.0122DePr}Pr$ works well for the flow rate range tested in asymmetric bifurcations (5.56 x 10^{-11} m^3/s to 2.78 x 10^{-10} m^3/s) with half angles θ_1 *and* θ_2 as 45º and 30º and channel diameter of 0.02m.

For the range of angles tested (θ_1 *and* θ_2 varying in pairs of 5º to 90º) the expression $L_{th} = 0.00035Pr^{0.2}De^{0.04}$ was the one that best fit.

The expression $L_{th} = \frac{1.8x10^{-8}+6.4x10^{-8}De^{0.5}Pr^{0.25}}{0.25+0.0488DePr}Pr$ was the format that best coincided with constant flow rate values (1.39 x 10^{-10} m/s) and half angles (θ_1 and θ_2 as 45º and 30º), with variation of pipe diameter between 0.01 and 0.035m.

For the case of variation of all parameters, the expression proposed as $L_{th} = \frac{3.3x10^{-8}+6.4x10^{-8}De^{0.5}Pr^{0.25}}{1+0.0122DePr}Pr$ was the best adapted as a correlation of broad aspect. It p resents some divergence for diameter variance, but coincides well with values that take into account the variation of half-angles and flow rates.

To conclude this cycle of studies, it is recommended to test the expressions in thermal flows involving variation of the properties that make up the Reynolds number

5. ACKNOWLEDGEMENTS

The authors acknowledge “Programa Pesquisa Produtividade - Universidade Estácio de Sá” for funding the research.

6. REFERENCES

Amado, F. P.; Avelino, M. R. ; Lucena. E. S. ; Colman, J., 2017. “The Region of not Fully Developed Flow in Bifurcations of Microchannels”. *Abstract in the proceedings of the IX Seminário de Pesquisa da Estácio e V Jornada de Iniciação Científica da UNESA*, Rio de Janeiro, Brasil;

Amado, F. P., Avelino. M. R., Colman, J., Lucena, E. S., Mazzarela, N. G. S., 2018a. “Developing Flow in the Inlet Region of Bifurcations in Microchannels with Symmetric Angulation”. *in the Proceedings of the Congresso Brasileiro de Engenharia Mecânica - CONEN2018*, Salvador, BA, Brasil. DOI: 10.26678 /ABCM.CONEM2018.CON18-0253;

Amado, F. P., Avelino. M. R., Colman, J., Lucena, E. S., Mazzarela, N. G. S., 2018b. “Forecasting the Length of the Undeveloped Flow Region in the Inlet of Asymmetric Bifurcations I”. *In the Proceedings of the 17th Brazilian Congress of Thermal Sciences and Engineering - ENCIT2018*, Águas de Lindóia, SP, Brazil. DOI://10.26678/ABCM.ENCIT2018.CIT18-0008;

Amado, F. P., Avelino. M. R., Colman, J., Lucena, E. S., Mazzarela, N. G. S., 2018c. “Forecasting the Length of the Undeveloped Flow Region in the Inlet of Asymmetric Bifurcations II”. *In the Proceedings of the 17th Brazilian Congress of Thermal Sciences and Engineerings - ENCIT2018*, Águas de Lindóia, SP, Brazil. DOI://10.26678/ABCM.ENCIT2018.CIT18-0009;

Amado, F. P., Avelino, M. R., Lucena. E. S., Mazzarela, N. G. S., 2018d. “Flow development in symmetric bifurcations of microchannels”. *Abstract in the Proceedings of the X Seminário de Pesquisa e I Mostra de Extensão da Estácio*, Rio de Janeiro, Brazil;

Amado, F. P., Avelino. M. R., Lucena. E. S., Mazzarela, N. G. S., 2018e. “Flow development in asymmetric bifurcations”. *Abstract In the Proceedings of the X Seminário de Pesquisa e I Mostra de Extensão da Estácio*, Rio de Janeiro, Brazil;

Amado, F. P., Corradi, V. H., Vegara, P. F. H., Mazzarela, N. G. S., Da Silva, W. A., 2019. “Influence of Low Reynolds Number in the region of flow development In bifurcations”. *To be published in the Proceedings of the 25th ABCM International Congress of Mechanical Engineering - COBEM2019, October 20-25*, Uberlândia, MG, Brazil;

Cheng K. C., and Akiyama, M. , 1970. “Laminar Forced Convection Heat Transfer in Curved Rectangular Channels”. Microfluid Nanofluid, Journal of Heat Transfer, vol. 13, pp. 471–490;

Choi, U. S., Talbot, L., and Cornet, E. , 1979. “Experimental Study of Wall Shear Rates in the Entry Region of a Curved Tube”. *Journal of Fluid Mechanics*, vol. 93, pp. 465–489;

Dravid, A. N., Smith, K. A., Merill, E. W., and Brian, L. T., 1971. “Effect of Secondary Fluid Motion on Laminar Flow Heat Transfer in Helically Coiled Tubes”. *AICHE Journal*, vol. 17, pp. 1114–1122;

Ebadian, M. A., Zheng, B., and Lin, C. X., 2000. “Combined Laminar Forced Convection and Thermal Radiation in a Helical Pipe”. *International Journal of Heat and Mass Transfer*, vol. 43, pp. 1067–1078;

Gongnan, X., Shian, L., Bengt S., Weihong, Z., and Haibin, L., 2014, “A numerical study of the thermal performance of microchannel heat sinks with multiple length bifurcation in laminar liquid flow”, Numerical Heat Transfer, Part A, 65: 107–126, DOI: 10.1080/10407782.2013.826084;

Ghobadi. M., Muzychka, Y. S., 2016. "A Review of Heat Transfer and Pressure Drop Correlations for Laminar Flow in Curved Circular Ducts", *Heat Transfer Engineering*, 37:10, 815-839, DOI: 10.1080/01457632.2015.1089735;

Janssen, L. A. M., and Hoogendoorn, C. J., 1978. "Laminar Convection Heat Transfer in Helical Coiled Tubes". *International Journal of Heat and Mass Transfer*, vol. 21, pp.1197–1206;

Liu, S., and Masliyah, J. H., 1994. "Developing Convective Heat Transfer in Helical Pipes With Finite Pitch". *International Journal of Heat and Fluid Flow*, vol. 15, no. 1, pp. 66–75;

Okuyade, W. I. A. and Abbey T. M., 2016 "Steady MHD Fluid Flow in a Bifurcating Rectangular Porous Channel". *Advances in Research.* 8(3): 1-17. DOI: 10.9734/AIR/2016/26399;

Soh, W. Y. and Berger, S. A., 1984. "Laminar Entrance Flow in a Curved Pipe". *Journal of Fluid Mechanics*, vol. 148, pp. 109–135;

So, R. M., Zhang, H. S. and Lai, Y. G., 1991. "Secondary Cells and Separation in Developing Laminar Curved-Pipe Flows". *Theoretical and Computational Fluid Dynamics*, vol. 3, no. 3, pp. 141–162;

Springer, F., Carretier, E., Veyret, D., Moulin, P., 2009. "Developing Lengths in Woven and Helical Tubes with Dean Vortices Flows". *Engineering Applications of Computational Fluid Mechanics*. 3:1. 123-134. DOI:10.1080/19942060.2009.11015259;

Stewartson, K., Cebeci, T. and Chang,K.C., 1980. "A Boundary Layer Collision in a Curved Duct". *The Quarterly Journal of Mechanics and Applied Mathematics*, vol. 33, pp. 59–75;

Stewartson,K.. and Simpson, C.J., 1982, 1982. "On a Singularity Initiating a Boundary-Layer Collision". *The Quarterly Journal of Mechanics and Applied Mathematics*, vol.35,pp.1–16;

Tarbell, J. M., and Samuels, M. R., 1973. "Momentum and Heat Transfer in Helical Coils". *Chemical Engineering Journal Lausanne (Netherlands)*, vol. 5, pp. 117–127;

Yao, L. S., 1984. "Heat Convection in a Horizontal Curved Pipe", *Journal of Heat Transfer*, vol. 106, pp. 71–77.

7. RESPONSIBILITY NOTICE

The authors are the only responsible for the printed material included in this paper.